SP-230—63

# Design and Construction of a Bridge Deck using Mild and Post-Tensioned FRP Bars

by R. Fico, N. Galati, A. Prota, and A. Nanni

**Synopsis:** The type of structure selected for this research project is a four-span continuous concrete slab having GFRP bars for top and bottom mats and CFRP reinforcement for internal post-tensioning. The bridge is located in Rolla, Missouri (Southview Drive on Carter Creek). One lane of the bridge was already built using a conventional four-cell steel reinforced concrete box culvert. One lane and sidewalk needed to be added and were constructed using FRP bars.
This study includes design of the FRP portion of the bridge using existing codes, validation of the FRP technology through a pre-construction investigation conducted on two specimens representing a deck strip, and construction of the bridge; the results showed how FRP, in the form of GFRP as passive and CFRP bars as active internal reinforcement, could be a feasible solution replacing the steel reinforcement of concrete slab bridges, and specifically the enhanced shear capacity of the slab due to the CFRP prestressing.

Keywords: anchoring systems; bridge deck; FRP tendons; post-tension

**Raffaello Fico** is a Ph.D student at the University of Naples Federico II, Italy. He performed his undergraduate thesis in collaboration with the University of Missouri-Rolla on the same topic of this paper. He was the supervisor of the installation of Southview bridge deck.

**Nestore Galati** is a research engineer at the University of Missouri–Rolla. He obtained is PhD in Civil Engineering at the University of Lecce-Italy where he also received his B.Sc. in Materials Engineering. He obtained his M.Sc. degree in Engineering Mechanics at the University of Missouri-Rolla. His research has concentrated on the area of retrofitting of masonry and upgrade and in-situ load testing of reinforced concrete structures. He is an EIT in the United States.

**Andrea Prota** is Assistant Professor of Structural Engineering at University of Naples Federico II, Italy. He is member of *fib* WG 9.3 and Associate Member of ACI 440 Committee. His research interests include seismic behavior of RC and masonry structures, use of advanced materials for new construction and for retrofitting of existing structures, and use of innovative techniques for structural health monitoring .

**Antonio Nanni** FACI, is the V & M Jones Professor of Civil Engineering at the University of Missouri – Rolla, Rolla, MO and Professor of Structural Engineering at the University of Naples, Italy. He was the founding Chair of ACI Committee 440, Fiber Reinforced Polymer Reinforcement, and is the Chair of ACI Committee 437, Strength Evaluation of Existing Concrete Structures.

## INTRODUCTION

Reinforced and prestressed concrete (RC and PC) structures are facing a worldwide problem, which is the corrosion of the steel as a result of aging and aggressive environments. Steel corrosion leads to member degradation, endangers structural integrity and may even cause catastrophic failures. Research has been carried out in an effort to find the solution for this problem. Fiber Reinforced Polymers (FRP), have been proposed for use in lieu of steel for reinforcement and prestressing tendons in concrete structures. The promise of FRP materials lies in their high-strength, lightweight and non-corrosive, non-conducting, and non-magnetic properties.

The interest in the use of FRP composites in prestressed concrete is mainly based on durability issues. Corrosion of prestressing steel tendons can cause serious deterioration of infrastructure. Properties like high tensile strength and high resistance to corrosion make FRP composites good candidates for prestressed and post-tensioned tendons.

Moreover, unlike steel reinforced concrete sections, members reinforced with FRP bars have relatively small stiffness after cracking. Therefore, serviceability requirements have also been examined.

## RESEARCH OBJECTIVES

The objectives of this research project were as follows:

1. Evaluate the feasibility, behavior and effectiveness of an innovative deck system, showing how glass and carbon FRP (GFRP and CFRP), in the form of passive and active internal reinforcement, could be a solution replacing steel reinforcement.
2. Provide analytical data in support of the enhanced shear capacity of the concrete slab due to the CFRP post-tensioning.

## DESCRIPTION OF THE PROJECT

The City of Rolla, MO has made available a bridge (Southview Drive on Carter Creek) to demonstrate the use of FRP bars and tendons in new constructions. One lane of the bridge was already constructed using conventional four-cell steel RC box culvert. It consists of a steel RC slab about 0.25 m thick, as depicted in Figure 1. The slab deck is continuous over three intermediate RC vertical walls, and the overall length of the bridge is roughly 12 m. The new deck was built on three conventional RC walls as for the existing structure. The construction of the FRP reinforced slab, plus a 2 m wide conventional RC sidewalk on the opposite side, allowed extending the overall width of the bridge from 3.9 m to 11.9 m, as Figure 2 shows. The construction of the bridge started on July 2004 and finished on October 2004.

## THEORETICAL ANALYSIS

The analysis and design of the FRP concrete bridge deck was based on the following assumptions:

- Nominal properties for FRP reinforcing material taken from the manufacturer published data and considered as initial guaranteed values to be further reduced to take into account the environmental reduction factors as given in ACI 440.1R-03;
- Load configurations consistent with AASHTO Specifications;
- Design carried out according to ACI 440.1R-03; and
- Effects due to the skew neglected.

The design properties of concrete and FRP bars used are summarized in Table 1.

### Summary of the structural analysis

Bending moments and shear forces are summarized in Table 2. Columns (1) and (3) represent the factors to be applied to dead and live load, respectively. Columns (2) and (4) show unfactored moment and shear, due to dead and live load, respectively.

### Flexural design

The flexural design of a FRP RC member is similar to the design of a steel RC member. The main difference is that both concrete crushing and FRP rupture are potential mechanisms of failure.

The ultimate flexural capacity of the bridge deck was calculated according to ACI 440.1R-03 using the following equation:

$$M_n = A_f \varepsilon_f E_f \left( d - \frac{\beta_1 c}{2} \right) + A_{fp} \varepsilon_{fp} E_{fp} \left( d_p - \frac{\beta_1 c}{2} \right) \tag{1}$$

where $A_f$ and $A_{fp}$ is the area of GFRP and CFRP reinforcement, respectively; $\varepsilon_f$ and $\varepsilon_{fp}$ their respective strains; $E_f$ and $E_{fp}$ the respective moduli of elasticity; $d$ and $d_p$ represents the distance from extreme compression fiber to the centroid of the tension GFRP and CFRP reinforcement, respectively. $\beta_1 c$ is the depth of the equivalent rectangular stress distribution in concrete.

Assuming the post-tensioned tendons strained at 65% of their ultimate capacity and a 35% of total losses, the theoretical moment capacity is found to be 64 kN-m. Since the failure mode is controlled by the rupture of the GFRP bars, the post-tensioning does not influence the moment capacity.

**Shear design**

The concrete contribution to the shear capacity, $V_{c,f}$, of the bridge deck was calculated according to ACI 440.1R-03 as follows:

$$V_{c,f} = \frac{A_f E_f}{A_s E_s} V_c \tag{2}$$

where $V_c$ represents the nominal shear strength provided by the concrete and the ratio $(A_f E_f / A_s E_s)$ takes into account the axial stiffness of the FRP reinforcement as compared to that of steel reinforcement. $A_s$ reported in Eq. (2) can be found by determining the area of steel reinforcement required to match the factored FRP flexural capacity, $\phi M_n$.

The concrete contribution to the shear capacity, $V_c$, was determined according to ACI318-99, sec. 11.4, which prescribes for post-tensioned members the following equation:

$$V_c = (0.05\sqrt{f_c^{'}} + 4.83\frac{V_u d_p}{M_u}) b_w d_p \tag{3}$$

Ultimate shear and moment laid out in eq.(3) are taken at a cross-section on the central support where both negative bending moment and shear force reach their maximum values, as summarized in Table 2.

The factored shear capacity is $\phi V_n = \phi V_{c,f} = 162 kN/m$ which is higher than the shear demand $V_u = 160.5\ kN/m$. If the post-tensioning action was not considered, the shear capacity would have been $\phi V_n = \phi V_{c,f} = 95 kN/m$ which is much smaller than the demand (the shear capacities have been computed from an analysis performed on the cross section flush with the vertical wall representing the support). The post-tensioning allowed an increase of shear capacity of more than 70%.

As an alternative approach to the shear capacity of the bridge deck, the following equation (Tureyen and Frosh 2003), now under consideration for adoption by ACI Committee 440, could be used:

$$V_{c,f} = \frac{2\sqrt{f_c^{`}}bc}{5} \tag{4}$$

where $c$ is the position of the neutral axis at service. Using such approach, the shear capacity would be *190.4 kN/m*.

**<u>Serviceability</u>**

Crack width, long-term deflection, creep rupture and fatigue have been also computed according to ACI 440. The slab was partially post-tensioned, thus permitting some tensile stresses at full service load.

Crack width of FRP reinforced flexural members can be expressed as suggested by ACI 440 as follows:

$$w = \frac{2200}{E_f}\beta k_b f_f \sqrt[3]{d_c A} \tag{5}$$

where $\beta$ is the ratio of the distance from the neutral axis to extreme tension fiber to the distance from the neutral axis to the center of tensile reinforcement, $k_b$ is a bond dependant coefficient equal to *1.2*, $f_f$ represents the stress at service in the FRP, $d_c$ is the thickness of the concrete cover measured from extreme tension fiber to the center of the bar, $A$ is the effective tension area of concrete defined as the area of concrete having the same centroid as that of tensile reinforcement, divided by the number of bars. The crack width of the slab, calculated with eq.(5), yields *w=0.0099 mm,* much smaller than the allowed value suggested by ACI 440 and equal to *0.5 mm*.

The long-term deflection can be calculated as suggested by ACI 440 as follows:

$$\Delta = \Delta_{LL} + \lambda(\Delta_{DL} + 0.2\Delta_{LL}) \tag{6}$$

where $\lambda = 1.2$ represents the multiplier for additional long-term deflection. Eq. (6) yields to $\Delta = 1.3mm$, smaller than the suggested AASHTO value of 3.8 mm.

To avoid creep rupture of the FRP reinforcement under sustained loads, the stress level in the FRP bar should be limited to the value suggested in ACI 440.1R.03. Specifically, when GFRP reinforcement is used, the stress limit has been set to be equal to $0.20\ f_f = 87\ MPa$.

The stress at service in the FRP is:

$$f_f = E_f \varepsilon_f = 16MPa \tag{7}$$

This value is much smaller than the allowable stress and therefore creep rupture and fatigue are not an issue for the long term behavior of the bridge.

## PRE-CONSTRUCTION INVESTIGATION

Two identical specimens representing a deck strip 457 mm wide, 254 mm deep and 7 m long, were fabricated and tested as continuous slabs over three supports (Galati et al., 2004). One specimen was used to investigate the flexural behavior ("flexural" specimen), while the other one the shear behavior ("shear specimen"). The testing allowed validating the design calculations both in terms of flexure and shear capacities.

The specimens had the same reinforcement percentage of the bridge deck: they were reinforced using 3 $\phi$19 GFPR bars as top and bottom mat and 2 $\phi$9 CFRP bars as post-tensioning tendons. The position of the tendons was varied along the specimen in order to match the moment demand. In addition, in order to reproduce the actual field conditions, also $\phi$13 GFRP bars spaced 305 mm on center were placed in the transverse direction Figure 3 shows a detailed layout of the specimens' reinforcement, while Figure 4 shows the position of the CFRP tendons.

### Test Setup

Each slab was tested as a continuous member on three supports, comprising of a 3.6 m and 1.8 m long span. The positions of the two loading points were chosen such to force flexural and shear failure for the flexural and shear specimens respectively. They were placed at the mid-spans for the flexural specimen (See Figure 5-a)), and 0.9 m away from the central support in the case of the shear specimen (See Figure 5-b)).

The flexural specimen was instrumented using three load cells: two of them were placed under the loading points while the third one was placed under one of the supports in order to determine the end reaction and therefore the real distribution of moments in the slab. Loads were applied to 102 x 457 x 25 mm steel plates resisting on the slab. The loads were generated by means of 30 ton hydraulic jacks reacting against a steel frame. The loading rate was the same for the two spans until reaching 85 kN. After that, the load in the shorter span was kept constant while the one in the longer one was increased until failure. This solution was adopted in order to avoid shear failure at the central support. Linear Variable Displacement Transducers (LVDTs) were positioned at the loading points (two for each loading point) and at the supports in order to record maximum displacements and support settlements. A total of 21 Electrical Strain Gages (ESG) were used to monitor the strain at the most critical sections. They were placed on each GFRP bar in correspondence with loading points and the central support. In addition, at the same locations, an additional strain gage was attached on the compressive face of the slab in order to have an additional backup point while determining the experimental moment-curvature response of the slab.

For the shear specimen, the number of load cells was reduced to two. Loads were applied to 102 x 457 x 25 mm steel plates resisting on the slab by means of a 100 ton hydraulic jack. Two additional LVDTs were inserted in order to also measure the maximum displacement which, in this case, was not at the loading points.

The load was applied in cycles of loading and unloading. An initial cycle for a low load was performed on every specimen to verify that both the mechanical and electronic equipment was working properly.

**Test results and discussion**

For the "flexure" specimen, the first flexural crack was observed on the longer span when the load was approximately 66 kN on both spans. As the loads were increased, some of the cracks started to extend diagonally to form shear cracks. At maximum loads, 163 kN and 100 kN for long and short spans respectively, concrete crushing at the top was observed. This was immediately followed by a sudden shear failure which also caused the rupture of the CFRP bars due to kinking (see Figure 6-a)).

The maximum bending moment was equal to 102 kN-m (when considering $C_E$=1, $\phi$=1), which compared to the theoretical value of 98 kN-m corresponds to an increase of about 4%.

For the "shear" specimen, the first crack was observed at a load approximately of 89 kN at the central support where the moment was maximum. As the load was increased, the newly formed cracks between the central support and the loading point started to extend diagonally to form a shear crack. The failure of the specimen occurred for an applied load equal to 273 kN due to diagonal tension shear (see Figure 6-b)).

The shear specimen presented a shear capacity equal to 142 kN, larger than the theoretical capacity found using the ACI 440.1R-03 (70 kN, with post-tensioning), with a percentage increase equal to 103%, and to 46% when considering the Tureyen and Frosh approach, confirming the conservative approach of ACI 440 for the shear.

## SOUTHVIEW BRIDGE DECK CONSTRUCTION

The slab is 0.25 m thick, 12 m long and 6 m wide. It is supported by three intermediate reinforced concrete vertical walls. The four span lengths are, from North to South, 2.89 m 3.38 m, 3.30 m and 2.35, respectively, on centers.

**Substructure construction**

The erection of the substructure and the extension of the existing abutments and walls were performed first. GFRP bars were inserted into the central wall in order to create a connection between the slab and the substructure (see Figure 7).

**Slab construction**

After laying the slab formwork, 13 mm thick neoprene pads were placed on the two abutments and on the two walls that did not have the GFRP anchoring rebars, in order to avoid restraining horizontally the slab and therefore to effectively post-tension it.Hence the bottom and the top layers of GFRP mild reinforcement were placed (see Figure 8).

A wooden board was built to make the slab end perpendicular to the tendons. This operation was performed in order to ease the post-tensioning phase (Figure 9). This was followed by the placing of plastic ducts to house the CFRP tendons. Such ducts were tied to the GFRP rebars; thirteen additional ducts were also placed (in case of imperfect post-tensioning), straight on the top side of the slab, as shown in Figure 10.

T connectors were used on each end of ducts in order to allow the injection of the grout after the pulling of the tendons. Strain gages were also attached on the longitudinal GFRP bars in order to monitor the slab during the service life. Figure 11 shows the bridge deck after pouring.

A week after the curing of the slab, the CFRP tendons were post-tensioned. The pulling was achieved by means of the jack already used for the specimens. Figure 12 shows the pulling device. It comprises an open steel box having enough room to push the wedges inside the chuck after pulling the tendon, a hydraulic jack to apply the pulling force, a round steel plate, a load cell to measure the load, a second plate and an outer chuck.

The steel wedge anchorage system used to lock in the CFRP bar and to react against the hydraulic jack was a three part system developed at the University of Waterloo, Canada. It included an outer steel cylinder, a four-piece wedge and an inner sleeve (see Figure 13). The inner sleeve was made out of copper to be deformable. The four-piece wedge was placed evenly around the inner sleeve and inserted into the outer steel cylinder. The anchorage system was later secured by tapping the inner sleeve and four-piece wedge into the outer steel cylinder with a special hammer.

The tendons were pulled at both terminations by means of two hydraulic jacks, connected to two pumps using load steps of 15-20 kN per side. The use of a single pump with two jacks connected in series was also considered, but it was not selected because it did not allow to ensure uniform load applications on the tendons. The applied load was measured using a data acquisition system connected to a computer allowing to monitor the applied load in real time.

After reaching the desired load the wedges were pushed inside the inner chuck, so each jack was released, engaging in such way the inner chucks. At this point FRP tendon was cut with an electric saw (see Figure 14).

The grout injection followed, after sealing the chucks to avoid grout leaking. After 4 days of curing the inner chucks were removed. Figure 15 shows a picture of the bridge after completion.

Finally, a barrier with GFRP reinforcement will be built on the new “FRP side”, in order to have a comparison during time with the steel reinforced concrete barrier on the opposite side, which is also going to be built. It will contribute to show the increased durability of a bridge deck using FRP materials as reinforcement, mainly due to the absence of corrosion.

## CONCLUSIONS

The following conclusions can be drawn:

- The post-tensioning allowed increasing the shear capacity of the slab by more than 70%. Moreover serviceability requirements are fully satisfied.
- The "shear" specimen presented a shear capacity much larger than the theoretical computed with the ACI 440.1R-03, confirming the very conservative approach of the guideline.
- The Tureyen and Frosh approach on shear appears to be less conservative than ACI 440.1R-03.
- Utilizing FRP in the form of reinforcing bars allows for the use of many steel-RC concrete practices. The fabrication and installation details were nearly identical to the methods regularly utilized for steel-reinforced slabs.
- The installation of the bridge highlighted the fact that having an efficient system is as important as having the adequate components. As well, for a new technology its learning curve must be overcome before its applications can be conducted proficiently.

## ACKNOWLEDGMENTS

The authors would like to acknowledge: the City of Rolla providing this opportunity and Dave Brown and Bill Cochran for their assistance in the different parts of the project; the financial support of the Missouri Department of Transportation, the University Transportation Center (UTC) at the University of Missouri–Rolla (UMR) for the research component of the project; Hughes Brothers for providing the FRP reinforcement; Jason Cox of Master Contractors LLC for reinforcement placement and post-tensioning.

## REFERENCES

**<u>Referenced standards and reports</u>**

The standards and reports listed below were the editions used for this project.

*AASHTO*

1994 Manual for Condition Evaluation of Bridges

1996 Design Code for Highway Bridges

2002 Standard Specifications for Highway Bridges, 17th Edition

*American Concrete Institute*

318-99 Building Code Requirement for Structural Concrete and Commentary

440.1R-03 Guide for the Design and Construction of Concrete Reinforced with FRP Bars

**Cited references**

Galati N, G. Boschetto, A. Rizzo, R. Parretti and A. Nanni, 2004: "Pre-Construction Investigation for the Rehabilitation of a Bridge Using Internal FRP Technologies," 4th International Conference on Advanced Composite Materials in Bridges and Structures - ACMBS-IV, July 20-23, 2004, Calgary, Alberta, Canada, CD-ROM version, 12

Hughes Brothers Inc, October 2003 "Hughes Brothers Reinforcements" Product Guide Specification, Web site: http://www.hughesbros.com.

Sika Corporation, July 2003, "SikaGrout 300 PT" Guide Specification, Web site: http://www.sikaconstruction.com.

Tureyen A. K. and Frosh R. J., 2003: "Concrete Shear Strength: Another Perspective", ACI Structural Journal, VOL. 100, NO.5 pp. 609-615.

## LIST OF NOTATIONS

$A$ = the effective tension area of concrete, defined as the area of concrete having the same centroid as that of tensile reinforcement, divided by the number of bars

$A_f$ = area of FRP reinforcement

$A_{fp}$ = area of post-tensioned FRP reinforcement

$A_s$ = area of steel reinforcement

$b$ = width of rectangular cross section

$b_w$ = width of the web

$c$ = distance from extreme compression fiber to the neutral axis

$C_E$ = environmental reduction factor for various fiber type and exposure conditions

$d$ = distance from extreme compression fiber to centroid of tension reinforcement

$d_c$ = thickness of the concrete cover measured from extreme tension fiber to center of bar or wire location closest thereto

$d_p$ = distance from extreme compression fiber to centroid of post-tensioned reinforcement defined as the mean modulus of a sample of test specimens

$E_f$ = guaranteed modulus of elasticity of FRP defined as the mean modulus of a sample of test specimens

$E_{fp}$ = guaranteed modulus of elasticity of post-tensioned FRP

$E_s$ = modulus of elasticity of steel

$f_c^{'}$ = specified compressive strength of concrete

$f_f$ = stress in the FRP reinforcement in tension

$k_b$ = bond-dependent coefficient

$M_n$ = nominal moment capacity

$M_u$ = factored moment at section,

$V_c$ = nominal shear strength provided by concrete with steel flexural reinforcement

$V_{c,f}$ = nominal shear strength provided by concrete with FRP flexural reinforcement

$V_n$ = nominal shear strength at section

$V_u$ = factored shear force at section

$w$ = crack width

$\beta_1$ = factor depending on the concrete strength

$\Delta$ = long term deflection

$\Delta_{DL}$ = deflection due to the dead load

$\Delta_{LL}$ = deflection due to the live load

$\varepsilon_f$ = strain in FRP reinforcement

$\varepsilon_{fp}$ = strain in post-tensioned FRP reinforcement

$\lambda$ = multiplier for additional long-term deflection

$\phi$ = strength reduction factor

Table 1- Design Material Properties

| Concrete Compressive Strength $f'_c$ (MPa) | FRP Internal Reinforcement Type | FRP Bar Size (mm) | FRP Tensile Strength $f^*_{fu}$ (MPa) | FRP Tensile Strain $\varepsilon^*_{fu}$ | FRP Modulus of Elasticity $E_f$(GPa) |
|---|---|---|---|---|---|
| 41.4 (Deck) | GFRP | $\phi$9 | 758 | 0.018 | 40.8 |
| | | $\phi$13 | 689 | 0.017 | 40.8 |
| | | $\phi$19 | 621 | 0.015 | 40.8 |
| | CFRP | $\phi$9 | 2068 | 0.017 | 124.1 |

Table 2 - Moment and Shear per Unit Strip (Live and Dead Load)

| Loading Conditions | Moment and Shear | Dead Load | | Live Load | | Ultimate |
|---|---|---|---|---|---|---|
| | | (1) | (2) | (3) | (4) | (5)=(1)(2)+(3)(4) |
| Design Truck | $M^+$ [kN-m/m] | $\gamma\beta_d$ (1) | 6.27 | $\gamma\beta_l$ (1) $(1+I^{(2)})$ | 29.69 | 92.09 |
| | $M^-$ [kN-m/m] | | 8.69 | | 23.52 | 77.56 |
| | Shear [kN /m] | | 4.92 | | 15.42 | 160.53 |
| Design Lane | $M^+$ [kN-m/m] | | 6.27 | | 18.21 | 59.41 |
| | $M^-$ [kN-m/m] | | 8.69 | | 17.29 | 59.88 |
| | Shear [kN /m] | | 4.92 | | 12.47 | 134.25 |

(1) Coefficients as per AASHTO (2002) Table 3.22.1A. For ultimate conditions: $\gamma$=(1.3); $\beta_d$=1.0; $\beta_l$=1.67

(2) Live load impact (0.3, assumed for design)

Figure 1—Views of the Former Bridge

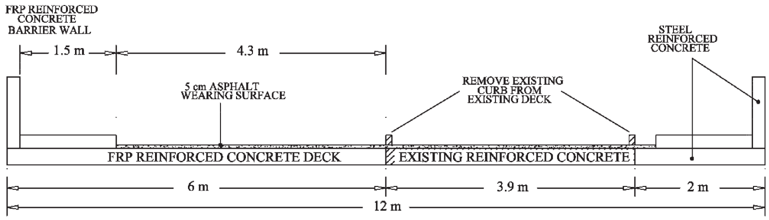


Figure 2—Cross Section of the Bridge After the Expansion

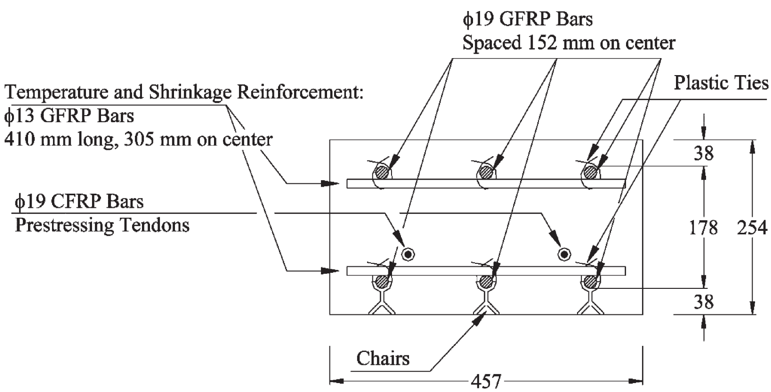


Figure 3—Specimen Reinforcement Layout

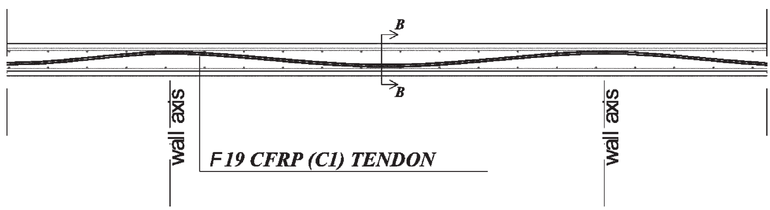


Figure 4—Longitudinal Section of the Slab for One of the Central Spans

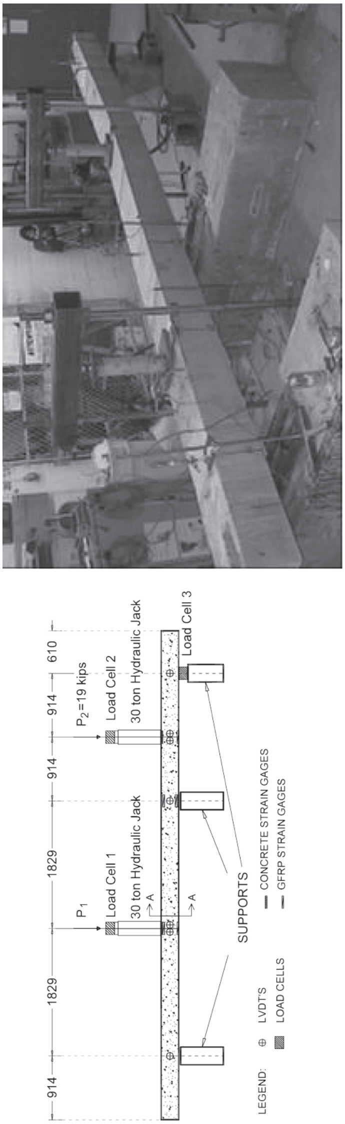


a) “Flexure” Test Setup

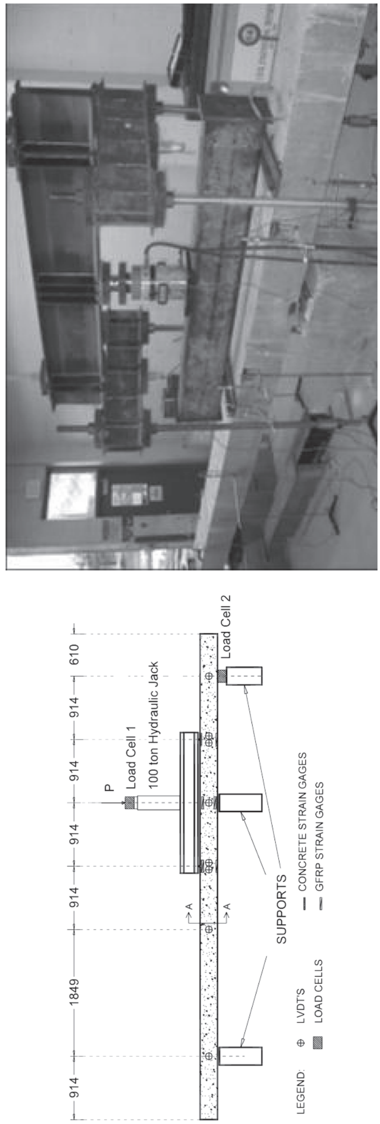


b) “Shear” Test Setup

Figure 5—Test Setups

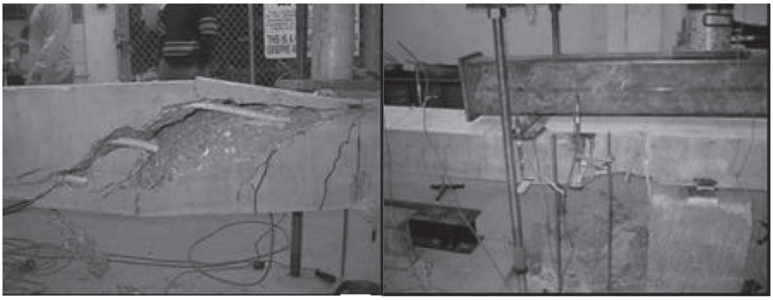

a) CFRP Bars Rupture Due to Kinking

b) Shear Cracks Near the Central Support

Figure 6—"Flexure and Shear Specimens" Failures

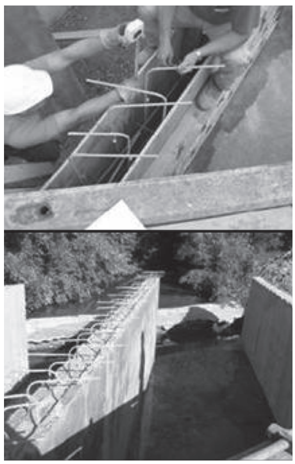

Figure 7—Placement of the GFRP Rebars into the Central Wall

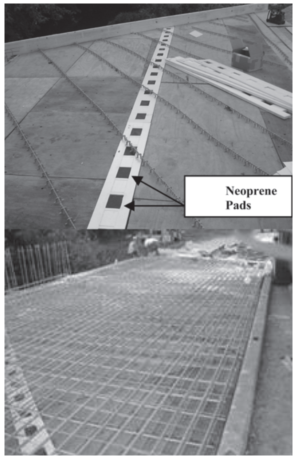


Figure 8—Neoprene Pads and GFRP Mild Reinforcement Details

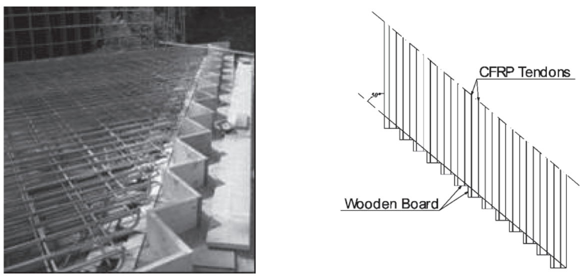


Figure 9—Wooden Board

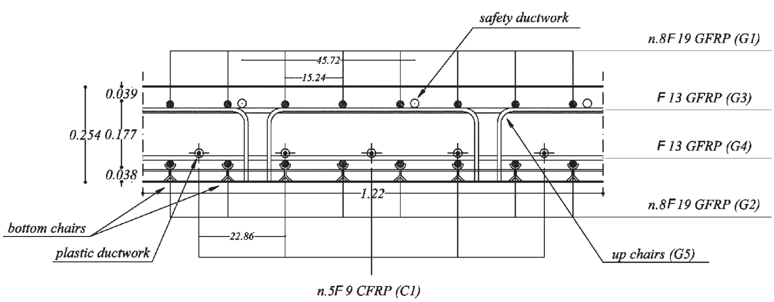


Figure 10—Slab Section B-B

Figure 11—Poured FRP Bridge Deck

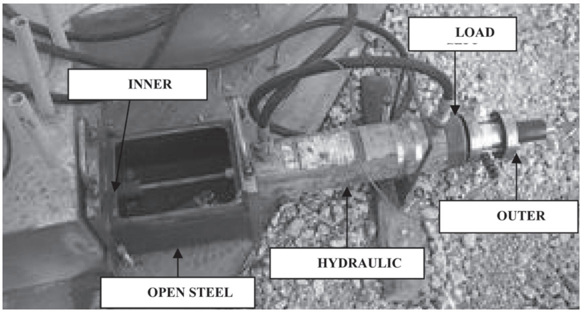


Figure 12—New Pulling Machine Ready for the Use

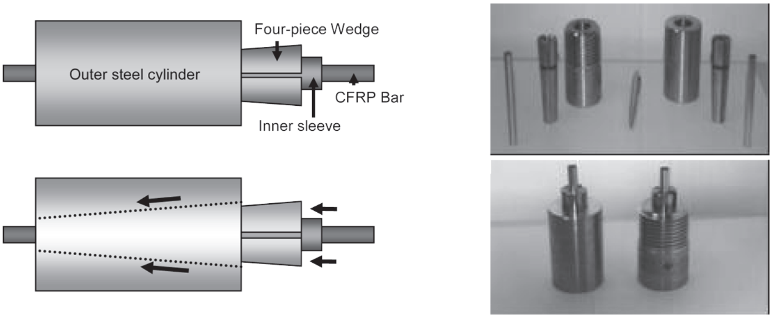


Figure 13—Steel Wedge Anchorage System

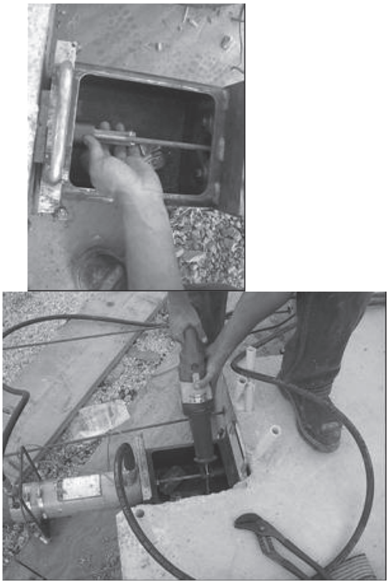

Figure 14—Wedges Insertion and Cutting of the Tendon

Figure 15—Southview Bridge-Deck Completed